ARTICLE

International Journal of
Applied Ceramic
TECHNOLOGY

3D mesoporous bioactive glass/silk/chitosan scaffolds and their compatibility with human adipose-derived stromal cells

Ratiya Buapa Phetnin[1] | Sanong Suksaweang[2] | Chiara Giannasi[3] | Anna Teresa Brini[3,4] | Stefania Niada[3] | Sawitri Srisuwan[1] | Sirirat Tubsungnoen Rattanachan[1] (iD)

[1]School of Ceramic Engineering, Institute of Engineering, Suranaree University of Technology, Nakhon Ratchasima, Thailand

[2]School of Pathology and Laboratory Medicine, Institute of Medicine, Suranaree University of Technology, Nakhon Ratchasima, Thailand

[3]IRCCS Istituto Ortopedico Galeazzi, Milan, Italy

[4]Department of Biomedical, Surgical and Dental Sciences, University of Milan, Milan, Italy

Correspondence
Sirirat Tubsungnoen Rattanachan, School of Ceramic Engineering, Institute of Engineering, Suranaree University of Technology, Nakhon Ratchasima, Thailand.
Email: sirirat.b@g.sut.ac.th

Funding information
Italian Ministry of Health; Suranaree University of Technology

Abstract

Human adipose-derived stem/stromal cells (hASCs) have been popularly studied as cell-based therapy in the field of regenerative medicine due to their ability to differentiate into several cell types. In this study, in order to improve the mechanical strength and bioactivity of scaffolds for bone tissue engineering, three types of mesoporous bioactive glasses with different shapes and compositions were dispersed in the silk fibroin/chitosan (SF/CS)-based scaffolds, which were fabricated with a combination of freezing and lyophilization. The characteristic and physical properties of these composite scaffolds were evaluated. The biocompatibility was also assessed through hASCs in vitro tests. Both Alamar Blue® and Live/Dead assay® revealed that the spherical mesoporous bioactive glass doped scaffolds enhanced cell viability and proliferation. Furthermore, the addition of spherical mesoporous bioactive glass into SF/CS scaffolds encouraged hASC osteogenic differentiation as well. These results suggested that this composite scaffold can be applicable material for bone regeneration.

KEYWORDS

bioactive glass, chitosan, composite scaffold, human adipose-derived stem/stromal cells, silk fibroin, tissue engineering

1 | INTRODUCTION

Bone regenerative materials have been studied by simulating the function and properties of natural tissues. After trauma, bone tumor resection, pathological fractures, and chronic bone infection, a graft replacement to restore bone's function may be needed.[1] Autografts are the gold standard for bone repair, but this method presents several limitations such as lacking sufficient transplantable materials, donor site morbidity, and resorption of the implanted bone. In addition, allografts and xenografts could lead to immunogenicity and entail the risk of immunological disease activation. Therefore, an ideal bone substitute should have natural-like properties containing hierarchical structures, good mechanical strength, and optimal biological properties. The three

main biological properties that should be taken into consideration are; osteoinduction, osteoconduction, and osteointegration to the surrounding bone. A combination of scaffolds and cells may overcome the loss of repairing of damaged bone tissue. Synthetic bone grafts should contain such pivotal qualities which are achieved by a combination of cells, scaffolds, and bioactive materials that can give functions of bioactive, biocompatible, and biodegradable properties. [2,3] Three-dimensional biodegradable scaffolds also play very important role in tissue engineering since they act as extracellular matrix (ECM) for cell attachment, migration, proliferation, and differentiation. In the field of biomaterials, scaffolds composed of both bioactive ceramics and biodegradable polymers have been gaining popularity due to their degradability, bioactivity, and strength.

Silk fibroin/chitosan (SF/CS) scaffold is a well-mixed natural polymeric scaffold with good biodegradability, biocompatibility, osteogenic inductivity, and safety.[4-6] However, the interaction between cells and the composite scaffolds remained to be unexplored and the osteogenic inductivity is still far from optimal need. Recently, mesoporous bioactive glass in the range of nanometer to micrometer size has emerged as a new class of bioactive glass with highly ordered interconnecting mesoporous structure characterized by various pore sizes ranging from 4 to 7 nm. The spherical mesoporous bioactive glass (SMBG) disperses much easier when combined with SF/CS scaffold than the irregular shaped mesoporous bioactive glass (MBG).[7] Also, SMBG provides higher surface area and pore volume, antibacterial properties,[8] and possesses drug delivery capacity. Moreover, the composite scaffold promotes in vitro apatite mineralization and degradation.[9] Zuk's group reported that Mesenchymal Stem/Stromal Cells (MSCs) harvested from adipose tissue were able to prolife rate on bioactive glass and further differentiate into adipocytes, chondrocytes, myocytes, and osteocytes under appropriate culture conditions.[10] In the last decades, adipose tissue has gained popularity as a source of MSCs for cell-based therapy due to the similar characteristics with bone marrow MSCs of both in vitro and in vivo[11] and a more convenient accessibility accounting for lower patient morbidity.However, there are no reports yet on the compatibility between human adipose-derived stem/stromal cells (hASCs) and the mesoporous bioactive glass/silk fibroin/chitosan scaffolds, nor on osteoinductivity. Here we investigated hASC viability, in vitro proliferation and osteogenic differentiation on three different composite scaffolds. In our study, mesoporous bioactive glasses, composed of 80 mol% SiO_2-15 mol% CaO-5 mol% P_2O_5 with different morphologies, were synthesized by the sol-gel method as previously described.[12] The irregular mesoporous bioactive glass (MBG), spherical mesoporous bioactive glass (SMBG), and 5% antibacterial doped mesoporous bioactive glass (5Ag-SMBG), were dispersed in SF/CS-based scaffolds before fabrication by lyophilization. Their characteristics, mechanical properties, and in vitro activity were finally investigated. In addition, the study of their biocompatibility with hASCs was also carried out in order to provide a proof of concept that they could be used as bone substitutes in regenerative medicine applications.

2 | MATERIALS AND METHODS

2.1 | Synthesis of irregular mesoporous bioactive glass (MBG) and spherical mesoporous bioactive glass (SMBG)

The mesoporous bioactive glasses were synthesized by the sol-gel method and denoted as irregular mesoporous bioactive glass (MBG), spherical mesoporous bioactive glass (SMBG)

and 5% Ag doped mesoporous bioactive glass (5Ag-SMBG). MBG and SMBG belong to the $80SiO_2 \cdot 15CaO \cdot 5P_2O_5$ system, according to previous publications.[7,13] 5Ag-SMBG, with silver as antibacterial addition, was synthesized by the sol-gel method as reported in our previous work.[12] The diameter of the particle ranged from 2 to 30 μm. MBG, SMBG, and 5Ag-SMBG presented a relative narrow pore size distribution, and the average pore diameters of all samples were between 4.3 and 5.3 nm which could be used as biological protein molecules or drug carriers.

2.2 | Fabrication of Silk fibroin/Chitosan (SF/CS), mesoporous bioactive glass/SF/CS composite scaffolds

Bombyx mori Thai silk (Nangnoi Srisaket 1) was supplied from Queen Sirikit Sericulture Center, Nakhon Ratchasima province, Thailand. Silk fibroin (SF) solution was prepared based on a previous method.[14,15] The concentration of SF solution was determined by weighing the remaining solid material after the completion of drying step.

Chitosan (CS) solution was prepared by dissolving 1 wt% chitosan in 2 wt% acetic acid before kept stirring at room temperature. The blending ratio of silk fibroin/chitosan in the composite scaffolds was studied in the preliminary study. The blending ratio of silk fibroin/chitosan was varied from 3:1, 2:2, and 1:3, respectively. The mechanical properties and morphology of the scaffolds were determined to find the optimal blending ratio. The compressive strength and compressive modulus gradually decreased when the concentration of chitosan was increased due to inferior mechanical properties of chitosan. The highest compressive strength was found for 3SF/1CS and the blending ratio of 3 silk fibroin:1 chitosan was selected with combination of MBGs in this study.

An equal volume of 3 wt% SF and 1 wt% CS solutions was mixed to fabricate the SF/CS scaffold. SF/CS scaffold was fabricated thoroughly by lyophilization and incubating it at −60°C for 24 hours to prefreeze the solution and continued with freeze-drying for 48 hours.

Three types of composite scaffolds were prepared from irregular mesoporous bioactive glass (MBG), spherical mesoporous bioactive glass (SMBG), and 5%Ag doped spherical mesoporous bioactive glass (5Ag-SMBG) in SF/CS scaffolds denoted as MBG/SF/CS,SMBG/SF/CS, and 5Ag-SMBG/SF/CS scaffolds respectively.All composite scaffolds were fabricated by mixing of 1% W/V mesoporous bioactive glass into the mixture of SF/CS solution prior to lyophilization as described above. All scaffolds were treated in methanol (99%) for 10-15 minutes and then lyophilized again for 24 hours. The preparation of the composite scaffolds is illustrated and shown in Figure 1.

2.3 | Characterization and testing of SF/CS scaffold and mesoporous bioactive glass/SF/CS composite scaffolds

2.3.1 | Chemical analysis

The diffraction patterns were recorded with XRD analyzer (Bruker Model D2) using Cu-Kα radiation (λ = 1.542 Å) at 35 kV and 40 mA. The samples were scanned in the interval of $10° < 2θ < 70°$ at a scan speed of 2°/min in a continuous mode. The chemical functional groups of the composite scaffolds were analyzed by Fourier transform infrared spectrometer (FT-IR; Bruker/Tenser27-Hyperion). The crushed scaffold samples were mixed with potassium bromide (KBr) and pressed into the pellets. The pellets were analyzed in the range of 400-4000 cm^{-1} and resolution of 4 cm^{-1}. The scaffolds were cut using a razor blade before sputtering coated with gold. The microstructure of the scaffolds was observed with a scanning electron microscope (SEM) at an acceleration voltage of 10 kV.

2.3.2 | Mechanical properties, porosity, and swelling ratio

Cylinder-shaped samples with 6 mm in diameter and 10 mm in height were tested according to the ASTM method F451-95. The compressive strength and Young's modulus of the composite scaffolds were determined by Computer-controlled Universal Testing Machine (UTM) with 0.1 kN load at room temperature. The crosshead speed was set at 0.5 mm/min. At least five replicates were carried out for each sample and the results were shown as mean ± SD.[16]

The porosity of the composite scaffolds was evaluated by Archimedes method. Hexane was used as the displacement liquid, as it is a nonsolvent for silk and chitosan, it is easily permeable through the interconnected scaffold pores, and it does not cause swelling or shrinkage. The scaffolds were immersed in hexane for 15 minutes. The dry weight of the composite scaffolds was recorded as W_1. The weight of the saturated scaffolds after soaking in hexane was recorded as W_2. The weight of submerged scaffolds in hexane was recorded as W_3. For all scaffold samples, the measures were carried out in triplicate.[17]

The porosity of the scaffold (ε) was calculated by:

$$\text{Porosity } (\%\varepsilon) = \frac{W_2 - W_1}{W_2 - W_3} \times 100\% \quad (1)$$

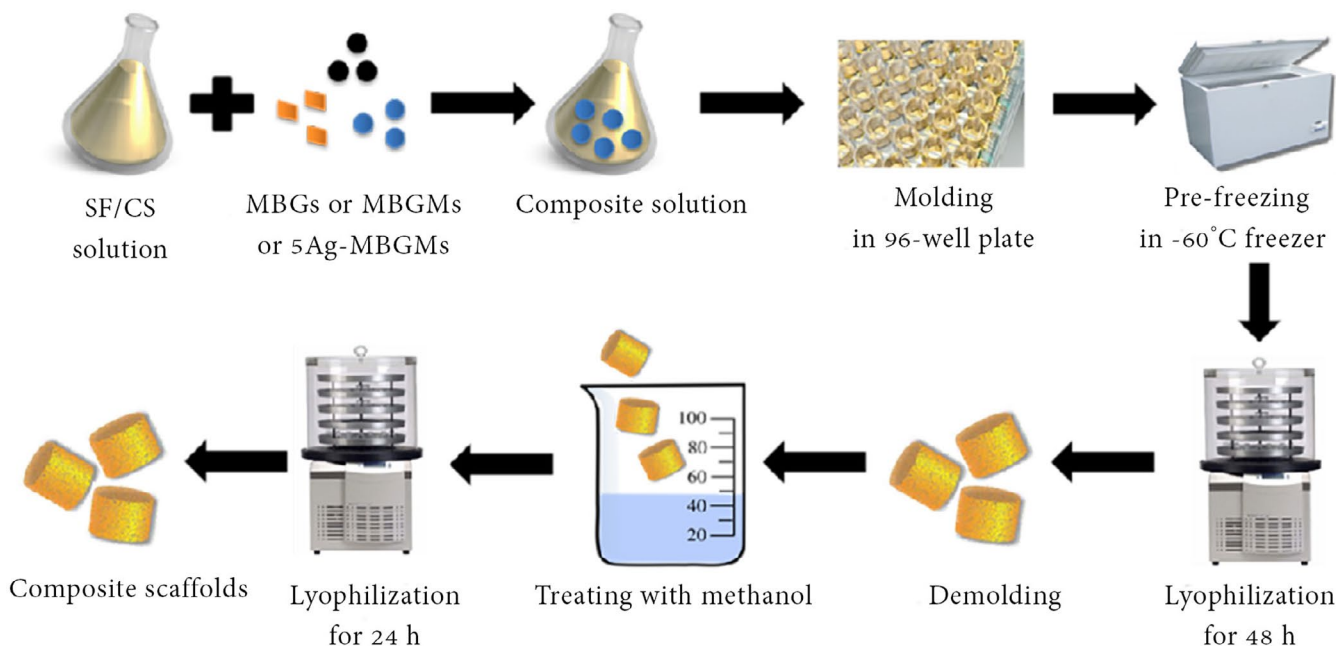Swelling measurement was provided with the distilled water at room temperature for 24 hours. Briefly, the dried scaffolds were weighed as W_d, and then immersed in 10 mL distilled water. After 24 hours of immersion, the soaked scaffolds were taken out carefully and weighed as W_s. The three repeating tests were provided for statistical data.[18]

The swelling ratio (Q) of these samples was calculated using the following equation:

$$\text{The swelling ratio } (Q) = \frac{W_s - W_d}{W_d} \quad (2)$$

2.3.3 | In vitro bioactivity assessment

Simulated body fluid (SBF) was prepared according to the procedure described previously.[19] Table 1 shows the comparison of ion concentrations of the SBF and human blood plasma.

SF/CS solution

MBGs or MBGMs or 5Ag-MBGMs

Composite solution

Molding in 96-well plate

Pre-freezing in -60˚C freezer

Composite scaffolds

Lyophilization for 24 h

Treating with methanol

Demolding

Lyophilization for 48 h

FIGURE 1 Schematic representation of the composite scaffold fabrication procedure [Color figure can be viewed at wileyonlinelibrary.com]

To determine the in vitro bioactivity of the composite scaffolds, they were immersed in the SBF solution and kept at 37°C. The SBF solution was changed every 2 days. After immersion for 7 days, the composite scaffolds were collected from SBF solution, rinsed with absolute ethanol, and air-dried at room temperature overnight. The samples were characterized by Field Emission Scanning Electron Microscope (FESEM) and Energy Dispersion X-Ray Spectrometer (EDS). The SBF solution was collected for determination of ion concentration changes of calcium, phosphate, silicon, and silver by Inductively Coupled Plasma Optical Emission Spectroscopy (ICP-OES) and reported as the mean ± SD. During time, the pH value of the SBF solution was also determined.

2.4 | In vitro biocompatibility of hASCs

2.4.1 | Isolation of hASCs

Adipose tissue was collected from the waste subcutaneous fat of healthy female donors undergoing plastic surgery at IRCCS Istituto Ortopedico Galeazzi, following the procedure PQ 7.5.125, version 4. Written informed consent was obtained from all donors. Primary cultures of the stromal vascular fraction (SVF) were established as previously described[10] and in Niada et al.[19,20]. Briefly, the fresh liposuction aspirates were washed at least three times with phosphate-buffered saline (PBS) supplemented with 150 U/mL penicillin and 150 μg/mL streptomycin and centrifuging at 1300 g for 2 minutes per cycle. Excess fluid containing red blood cells and PBS were removed with a Pasteur pipette. The matrix was enzymatically digested with 0.075% type I collagenase (Worthington, Lakewood, NJ, USA) at 37°C with continuous agitation for 30 minutes. The SVF was then centrifuged (1300 g, 10 minutes) and filtrated through a sterile cell-strainer (pore size: 100 μm). The collected SVF cells were plated in control medium (Dulbecco's modified Eagle medium [DMEM] + 10% fetal bovine serum supplemented with 50 U/mL penicillin, 50 μg/mL streptomycin, and 2 mM L-glutamine) at a seeding density of approximately 10^5 cells/cm². The cells were incubated at 37°C in a humidified atmosphere with 5% CO_2. After 48 hours, nonadhering cells were removed, and the medium was changed every other day. Adhering cells were grown until 80% confluence, then trypsinized using 0.5% trypsin/0.2% EDTA (Ethylene Diamine Tetra Acetic Acid). Cells at passage 3 through 7 were used for all experiments.

2.4.2 | Cell seeding on the composite scaffolds

Dry composite scaffolds were cut into 6 mm in diameter and 5 mm in thickness and sterilized in oven at 140°C for 2.5 hours. Scaffolds were prewetted in serum free DMEM overnight and, then 5×10^4 undifferentiated hASCs, resuspended in 50 μL of culture medium, and were seeded on to each composite scaffold. Cells were allowed to adhere for 3 hours, and then 1 mL of culture medium was added to the constructs. The cell-composite scaffolds were incubated in either control or osteogenic medium (OSTEO:control medium supplemented with 10 nM dexamethasone, 10 mM glycerol-2-phosphate, 150 μM L-ascorbic acid-2-phosphate, 10 nM cholecalciferol, Sigma-Aldrich) to investigate the osteogenic differentiation potential for up to 14 days, with media changing every other day.

2.4.3 | Cell viability and proliferation

The first screening of the biocompatibility between hASCs and the four different scaffolds was performed using a GFP-expressing cell line (GFP⁺hASCs), kindly provided by Dr Giulio Alessandri of IRCCS Neurological Institute Carlo Besta, Milan.[21] The green fluorescent protein GFP has been widely used to track cells in a variety of applications. Cell viability and proliferation were determined by AlamarBlue® assay based on metabolically active cells within each scaffold. AlamarBlue® assay was selected over MTT assay because it is a nontoxic method that allows monitoring the cell growth of a sample continuously through time. Briefly, seeded cells were cultured for different time spans and then incubated with 1 mL of 10% AlamarBlue® reagent in culture medium at 37°C with 5% CO_2. After 3.5 hours, supernatants were quantified for fluorescence intensity (540 nm excitation λ, 600 nm emission λ) by Wallac Victor II plate reader (PerkinElmer, Milan, Italy). Background fluorescence from AlamarBlue® solution alone was subtracted. In order to indirectly quantify the number of GFP⁺hASCs growing on the scaffolds overtime, a standard curve of cells seeded on cell culture plastic was set, analyzed by AlamarBlue®, and used to interpolate the data obtained on the different scaffolds.[22] Since the constitutive expression of fluorescent proteins enables to directly track cells, we harnessed this feature to monitor

TABLE 1 Ion concentrations of SBF and human blood plasma [19]

Types	Ion concentration (mM)							
	Na⁺	K⁺	Mg²⁺	Ca²⁺	Cl⁻	HCO₃⁻	HPO₄²⁻	SO₄²⁻
SBF	142	5	1.5	2.5	147.8	4.2	1	0.5
Blood plasma	142	5	1.5	2.5	103	27	1	0.5

cell attachment within the three-dimensional composite scaffolds by fluorescence microscopy.

At last, to evaluate the cell distribution and viability inside the composite scaffolds, Live/Dead® (Invitrogen Corporation, Carlsbad, CA) assay was also performed on primary hASCs following standard procedures.

2.4.4 | Osteogenic differentiation

To assess the osteogenic differentiation of hASCs on the composite scaffolds, alkaline phosphatase (ALP) activity was measured. About 5×10^4 cells were seeded onto each scaffold and cultured in either CTRL or OSTEO medium for 14 days. The cell-composite scaffolds were washed in PBS several times and then cells were lysed in 0.1% Triton® X-100 at 4°C for 30 minutes with three cycles of freeze-thawing. After centrifugation at 14 000 g for 15 minutes, supernatants were collected and their protein content was quantified by BCA assay (Pierce, Milan, Italy). Lysates were incubated with 10 mM p-nitrophenyl phosphate dissolved in 100 mM diethanolamine and 0.5 mM $MgCl_2$, pH 10.5 at 37°C until the colorimetric reaction occurred, then read at 405 nm. Experimental data were interpolated in a standard curve of known concentrations of p-nitrophenol (pNP, Sigma-Aldrich). ALP activity was expressed as U/μg of protein.

2.4.5 | Histology

After 14 days of culture, the cell-composite scaffold constructs were harvested. Samples were washed in PBS, fixed with 10% neutral buffered formalin (at 4°C 24 hours), dehydrated in graded ethanol solutions and impregnated with paraffin overnight. Then, paraffin sections of 5 μm were cut and collected on slides. Slides were stained with Hematoxylin and Eosin (H&E) for histological evaluation.

2.5 | Statistical analysis

The data were expressed as means ± SD for all experiments and were analyzed using a t test analysis. A value of $P \leq .05$ was considered statistically significant.

3 | RESULTS

3.1 | Characterization of mesoporous bioactive glass/SF/CS composite scaffolds

To evaluate the phase analysis, X-ray diffraction patterns of the composite scaffolds were examined as shown in Figure 2.

All composite scaffolds showed the characteristic peaks at 2θ around 21-23°, corresponding to the β-sheet crystalline structure of silk fibroin together with crystal structure of the anhydrous form of chitosan. This result indicated that both SF and CS existed in all composite scaffolds. Furthermore, the 5Ag-SMBG/SF/CS composite scaffold showed the intense broad peaks at 2θ to about 32-33°, corresponding to the crystallization of calcium phosphate and pseudo-wollastonite. In addition, the small typical peak of metallic silver was found in 5Ag-SMBG/SF/CS composite scaffolds.

Figure 3 shows FT-IR spectra of the different composite scaffold. In the composite scaffolds were found the absorption bands at 1626 (amide I), 1522 (amide II), 1233 (amide III), and 665 cm^{-1} (amide V), which were attributed to the β-sheet conformation of silk fibroin. On the other hand, chitosan characteristic absorption bands at 1156 and 875 cm^{-1} represented the saccharide structure. Additionally, bands at 1555 and 1655 cm^{-1} were known as the amino group of chitosan and the amide group of chitins, respectively. The double amide peaks for chitosan corresponded to the partial N-deacetylation of chitin. The peaks at 1415 cm^{-1} corresponded to carboxyl (–COOH) stretching bands. More importantly, all composite scaffolds showed the interaction of silk fibroin and chitosan bands at 1077 and 1043 cm^{-1}. FT-IR spectra of MBG/SF/CS, SMBG/SF/CS, and 5Ag-SMBG/SF/CS composite scaffolds also showed characteristic absorption bands of Si–O–Si bonds (dashed line) at 1062 (stretch vibration), 802 (bending vibration), and 450 cm^{-1} (bending vibration). The composite scaffolds exhibited the characteristic absorption bands of silk fibroin, chitosan, and mesoporous bioactive glass phases with different intensities varying due to the compositions of materials.

The architecture of all scaffolds was a three-dimensional interconnected structure with homogeneous pore size as
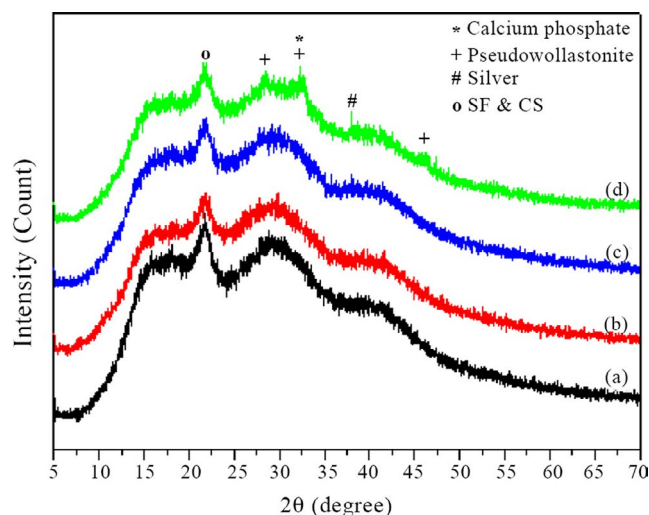
FIGURE 2 XRD patterns of (A) SF/CS, (B) MBG/SF/CS, (C) SMBG/SF/CS, and (D) 5Ag-SMBG/SF/CS composite scaffolds [Color figure can be viewed at wileyonlinelibrary.com]

shown in Figure 4. SEM images with high magnification indicated that the MBG, SMBG, and 5Ag-SMBG particles were found in the pore walls of the composite scaffolds (see arrows). The structure of the composite scaffolds was not significantly changed as compared to that of SF/CS scaffolds. The incorporation of MBG might collapse the structure of

the composite scaffold due to their larger particle size (up to 45 μm) as compared to SMBG and 5Ag-SMBG.[7] The range of pore size of the composite scaffolds was from several tens to hundreds of micrometers.

3.2 | Mechanical properties, porosity, and swelling ratio

The compressive strength, Young's modulus of the composite scaffolds, porosity, and swelling ratio are shown in Table 2. The highest compressive strength and Young's modulus were found for both SMBG/SF/CS and 5Ag-SMBG/SF/CS composite scaffolds followed by MBG/SF/CS and SF/CS scaffolds, respectively. Similar pattern was also found for Young's modulus of the composite scaffolds. The porosity of MBG/SF/CS scaffold was significantly increased as compared with other scaffolds. The SMBG addition in the SF/CS scaffold did not affect the porosity, whereas it improved the compressive strength and Young's modulus of the composite scaffolds.

The diffusion of liquid into the composite scaffolds was a necessary parameter related to the transportation of nutrients and oxygen inside. The swelling ratios of the composite scaffolds containing mesoporous bioactive glasses were significantly decreased as compared to SF/CS scaffolds.
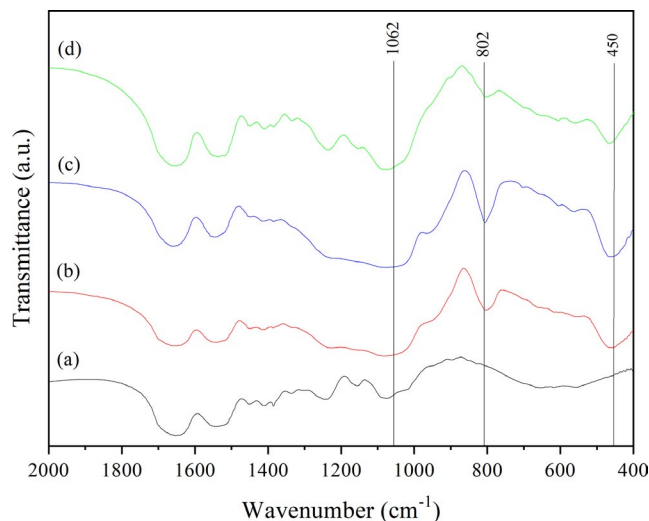
FIGURE 3 FT-IR spectra of (A) SF/CS, (B) MBG/SF/CS, (C) SMBG/SF/CS, and (D) 5Ag-SMBG/SF/CS scaffolds [Color figure can be viewed at wileyonlinelibrary.com]
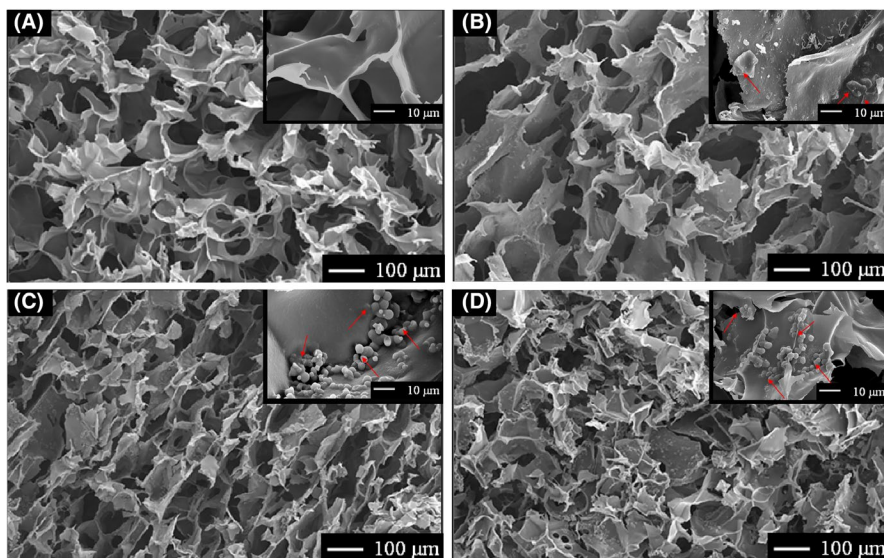
FIGURE 4 SEM micrographs of the different composite scaffolds (A) SF/CS, (B) MBG/SF/CS, (C) SMBG/SF/CS, and (D) 5Ag-SMBG/SF/CS [Color figure can be viewed at wileyonlinelibrary.com]

TABLE 2 Mechanical properties, porosity, and swelling ratio of the composite scaffolds

Types of scaffolds	Porosity (%)	Compressive strength (kPa)	Young's modulus (MPa)	Swelling ratio (%)
SF/CS	91.7 ± 0.99	230 ± 2	0.82 ± 0.03	34 ± 10
MBG/SF/CS	96.5 ± 0.45	250 ± 2	1.17 ± 0.03	23 ± 8
SMBG/SF/CS	91.9 ± 0.96	450 ± 1	2.39 ± 0.04	27 ± 10
5Ag-SMBG/SF/CS	92.2 ± 0.90	440 ± 0.5	2.35 ± 0.05	26 ± 8

PHETNIN ET AL.

International Journal of
**Applied
Ceramic**
TECHNOLOGY

| 2785

3.3 | Ion releasing and pH variations

The ICP analysis of the chemical species released from the composite scaffolds during 0-14 days are shown in Figure 5. The changes of the Ca and P ion concentrations in SBF showed a similar pattern for MBG/SF/CS and 5Ag-SMBG/SF/CS scaffolds. The Ca and P ions concentration increased at first 24 hours, and then gradually decreased to a certain value after 7 days as shown in Figure 5A and B. For all the composite scaffolds except from SF/CS, released Si ions reached a plateau after 7 days and then maintained it for the remaining immersion time. As expected, Ag ion release in SBF was only found in 5Ag-SMBG/SF/CS composite scaffolds. The ICP analysis of Ag ion concentration demonstrated that Ag ions were rapidly released within the first 24 hours of immersion, then reached a plateau until the end of the test. The releasing of Ag ion in 5Ag-SMBG/SF/CS composite scaffolds suggested that the composite scaffold may exert antibacterial properties. Figure 6 shows the pH variation of the SBF solution during 2 weeks of the

composite scaffolds immersion. The pH value of the composite scaffolds slightly decreased after immersion for 3 days while that of SF/CS scaffolds was rapidly decreased reaching pH values that can negatively affect cell behavior and/or survival.

3.4 | In vitro bioactivity

The FESEM observations further support the formation of calcium phosphate on the pore wall of the composite scaffolds. Figure 7 shows FESEM images of all composite scaffolds after immersion for 7 days in SBF solution. Before immersion in SBF solution, all composite scaffolds with different compositions showed smooth and homogeneous surface. After immersion for 7 days, some tiny particles consisting of rod-like and needle-like shape were observed on the surface of MBG/SF/CS and SMBG/SF/CS composite scaffolds, similar to the morphology of the precipitated calcium phosphate in human bones. This result indicated that
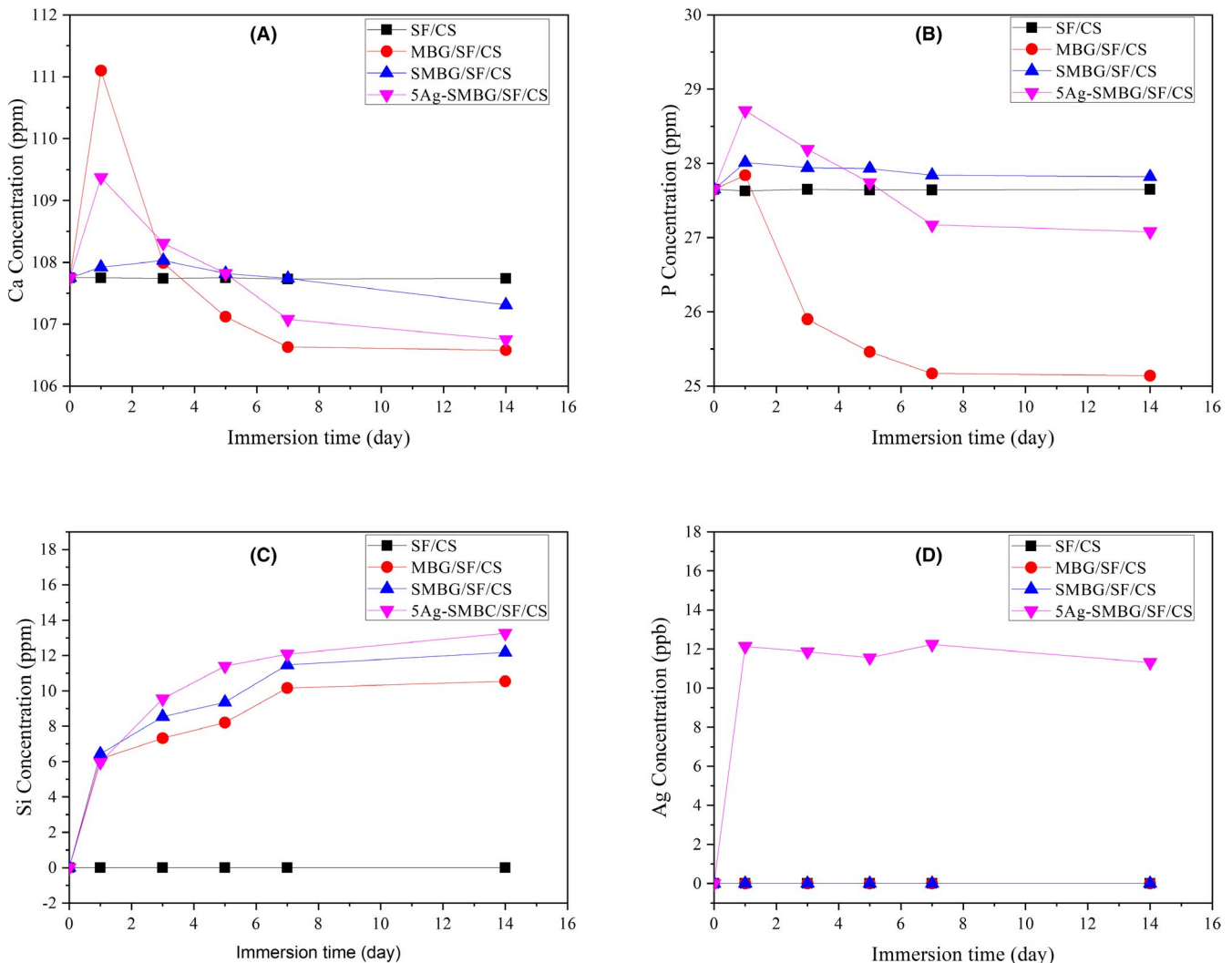

FIGURE 5 Concentrations of ions (A) Ca, (B) P, (C) Si, and (D) Ag released from the SF/CS, BG/SF/CS, SMBG/SF/CS, and 5Ag-SMBG/SF/CS scaffolds during immersion in SBF at 37°C for several days [Color figure can be viewed at wileyonlinelibrary.com]
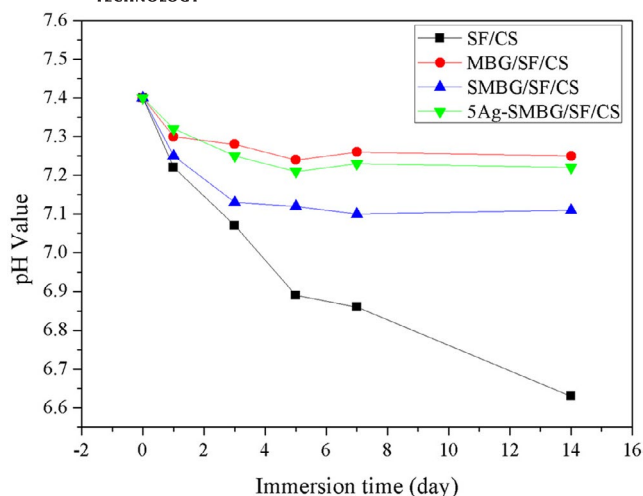
FIGURE 6 pH variation of SBF with the immersion times [Color figure can be viewed at wileyonlinelibrary.com]

the formation of the precipitated calcium phosphate was decreased for 5Ag-SMBG/SF/CS composite scaffolds, while no formation of the precipitated calcium phosphate on the SF/CS scaffolds appeared on the smooth surface. The EDS analysis of all composite scaffolds showed the presence of silicon, calcium, and phosphorus concentrations corresponding to mesoporous bioactive glass particles distributed on the pore wall of all the scaffold structures except the SF/CS ones. In addition, the 5Ag-SMBG/SF/CS composite scaffolds also showed the presence of silver corresponding to this metal doping in SMBG. The EDS analysis of the composite scaffolds after immersion in SBF solution showed that the Ca/P ratio on surface of the SF/CS, MBG/SF/CS, SMBG/SF/CS, and 5Ag-SMBG/SF/CS composite scaffolds were 0, 1.67, 1.56, and 1.62, respectively. The FESEM micrographs and EDS analysis revealed the deposition of calcium phosphate on the pore wall of the composite scaffolds in the following
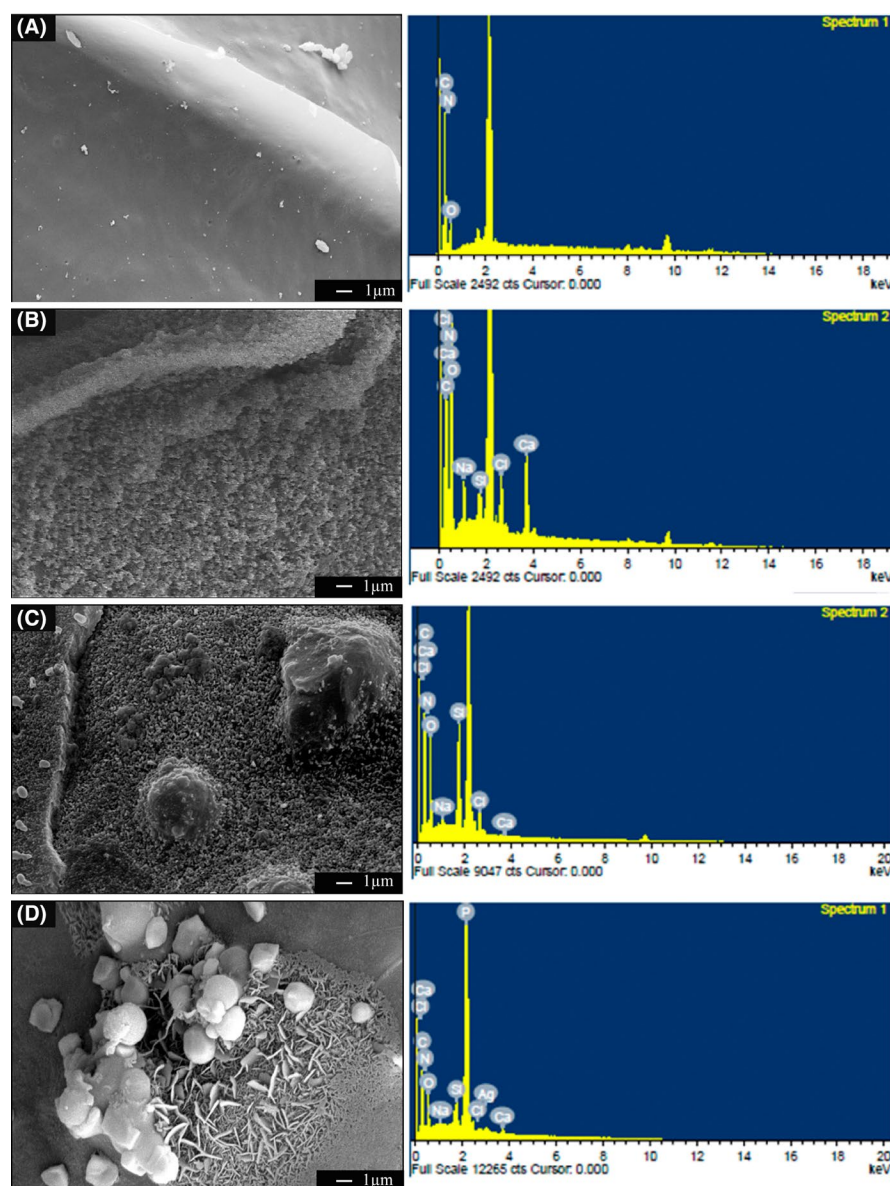
FIGURE 7 FESEM micrographs and EDS spectra of (A) SF/CS, (B) MBG/SF/CS, (C) SMBG/SF/CS, and (D) 5Ag-SMBG/SF/CS scaffolds after immersion in SBF solution for 7 days at 37°C [Color figure can be viewed at wileyonlinelibrary.com]

sequence MBG/SF/CS > SMBG/SF/CS > 5Ag-SMBG/SF/CS > SF/CS.

3.5 | Cell viability and proliferation

In this study, hASC proliferation and differentiation toward osteoblast-like cells on mesoporous bioactive glass/SF/CS composite scaffolds were investigated. For preliminary study, four types of composite scaffolds were seeded with green fluorescent protein expressing ASCs (GFP⁺hASCs).

During the first stage of seeding (time point = 3 days), the proliferation of GFP + hASCs loaded on composite scaffolds decreased because nonattached/dead cells were removed during the media changes. Then, cell proliferation increased during time except for the 5Ag-SMBG/SF/CS composite scaffolds. SMBG/SF/CS composite scaffold showed the best performance (Figure 8). The number of
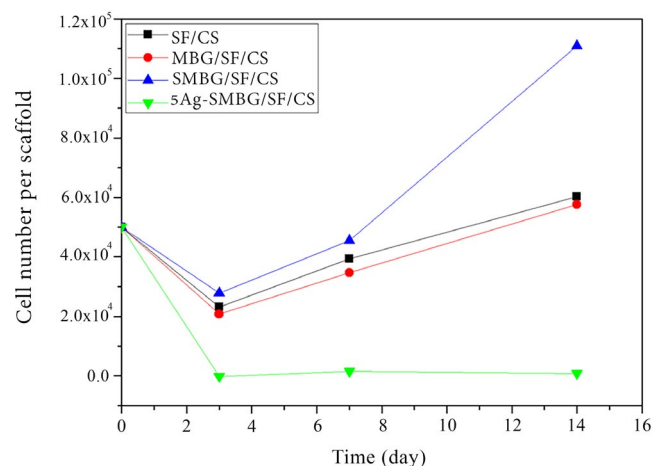
FIGURE 8 Cell proliferation on the composite scaffolds at different period of times (3, 7, and 14 days) by Alamar Blue® assay [Color figure can be viewed at wileyonlinelibrary.com]

cells in SF/CS scaffold was lower than that of the MBG/SF/CS and SMBG/SF/CS composite scaffolds. The attachment and spreading of GFP⁺hASCs on the composite scaffolds were confirmed by fluorescence microscopy as shown in Figure 9. After 14 days, hASCs were homogeneously increased for most of the scaffold surfaces, except for Ag-containing ones. Again, the most promising performance was obtained with SMBG/SF/CS scaffolds, suggesting that the compatibility of cell-composite scaffolds could be improved by the addition of mesoporous bioactive glasses. The 5Ag-SMBG/SF/CS scaffold was excluded in the further experiments due to its low biocompatibility and providing an unsuitable environment for cell growth and proliferation.
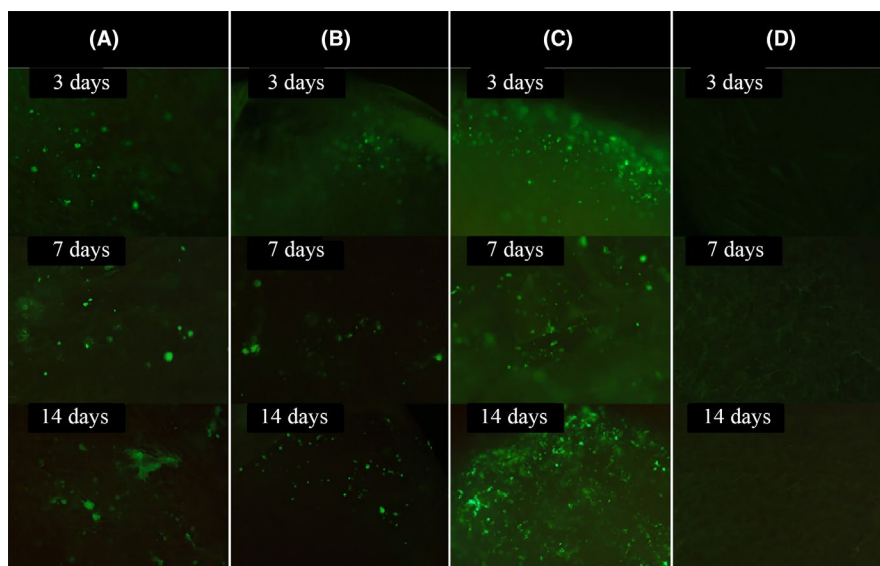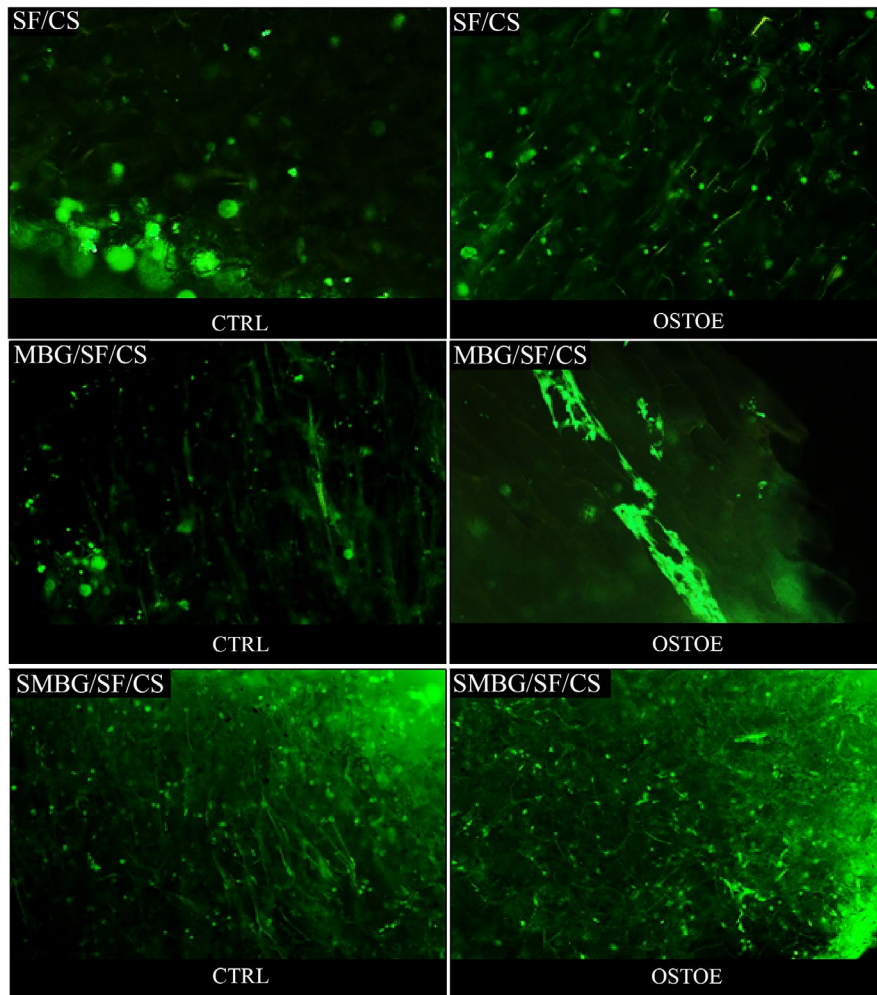
3.6 | Cell viability

hASCs were stained with Live/Dead® after 14 days of culture in CTRL or OSTEO medium and then observed under fluorescence microscopy. After 14 days in culture, most cells presented green fluorescence indicating they are viable, while almost no dead cells (red fluorescence) were found inside the composite scaffolds (Figure 10). Viable cells were found attached to the pore walls of all composite scaffolds. Once again, a higher number of cells was found in SMBG/SF/CS composite scaffold compared to the others, regardless of the type of culture medium (CTRL or OSTEO).

3.7 | Alkaline phosphatase activity

Alkaline phosphatase (ALP) activities of hASCs cultured on the composite scaffolds for 14 days in either CTRL or OSTEO medium were analyzed (Figure 11). As expected, ALP being a marker of osteoblasts, its activity levels were higher in all the samples cultured in osteogenic medium (OSTEO) compared

FIGURE 9 Fluorescence images of cells seeded on the composite scaffolds at different time points (3, 7, and 14 days). (magnification 40×); (A) SF/CS, (B) MBG/SF/CS, (C) SMBG/SF/CS, and (D) 5Ag-SMBG/SF/CS scaffolds [Color figure can be viewed at wileyonlinelibrary.com]

FIGURE 10 Fluorescence images of cell viability and cell distribution in the composite scaffolds after 14 days of culture in CTRL or OSTEO medium. Green color represents live cells (magnification = 40×) [Color figure can be viewed at wileyonlinelibrary.com]

to their appropriate counterparts (CTRL).In addition, ALP activity of hASCs cultured in OSTEO medium on MBG/SF/CS scaffold was higher than those cells osteo-differentiated on other scaffolds. Interestingly, also the ALP activity of cells grown on MBG/SF/CS scaffold under standard conditions (CTRL) was slightly higher than that assessed on SF/CS and SMBG/SF/CS, suggesting that the presence inside the SF/CS matrix of mesoporous bioactive glass particles with irregular shape, more than spherical ones, accounts for the better osteoinductive and osteoconductive properties of this scaffold and acts in synergy with the chemical cues present in the osteogenic medium.

3.8 | Histology

Histological evaluations by staining with hematoxylin and eosin (H&E) at 14 days revealed that the distribution of osteoinduced-hASCs in the composite scaffolds was better than control cells (Figure 12). Nevertheless, hASCs were distributed inside all the composite scaffolds, suggesting that all of them could represent suitable environment for hASCs growth, providing sufficient nutrients and gas exchange.
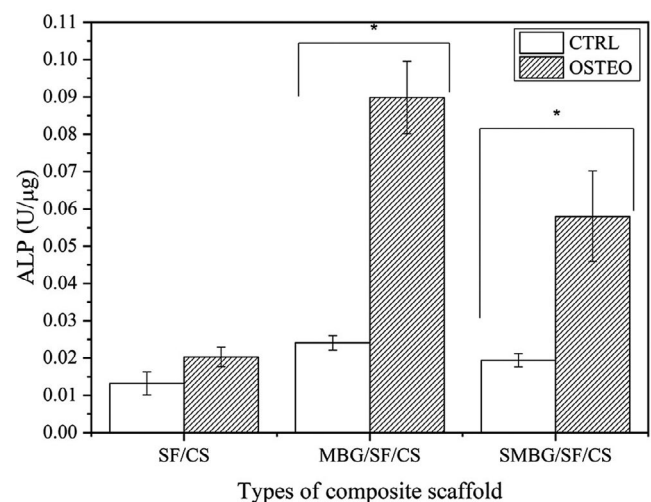

FIGURE 11 ALP activity of hASCs cultured on different composite scaffolds for 14 days in CTRL medium and OSTEO medium (seeding density: 5×10^4 cells/scaffold)

4 | DISCUSSION

In this study, the composite scaffolds were prepared from

PHETNIN ET AL.

Applied
Ceramic
TECHNOLOGY

International Journal of

2789

FIGURE 12 H&E staining of hASCs cultured in SF/CS, MBG/SF/CS, and SMBG/SF/CS composite scaffolds for 14 days in control (CTRL) and osteogenic (OSTEO) medium. Arrow heads point to hASCs (magnification = 40×) [Color figure can be viewed at wileyonlinelibrary.com]
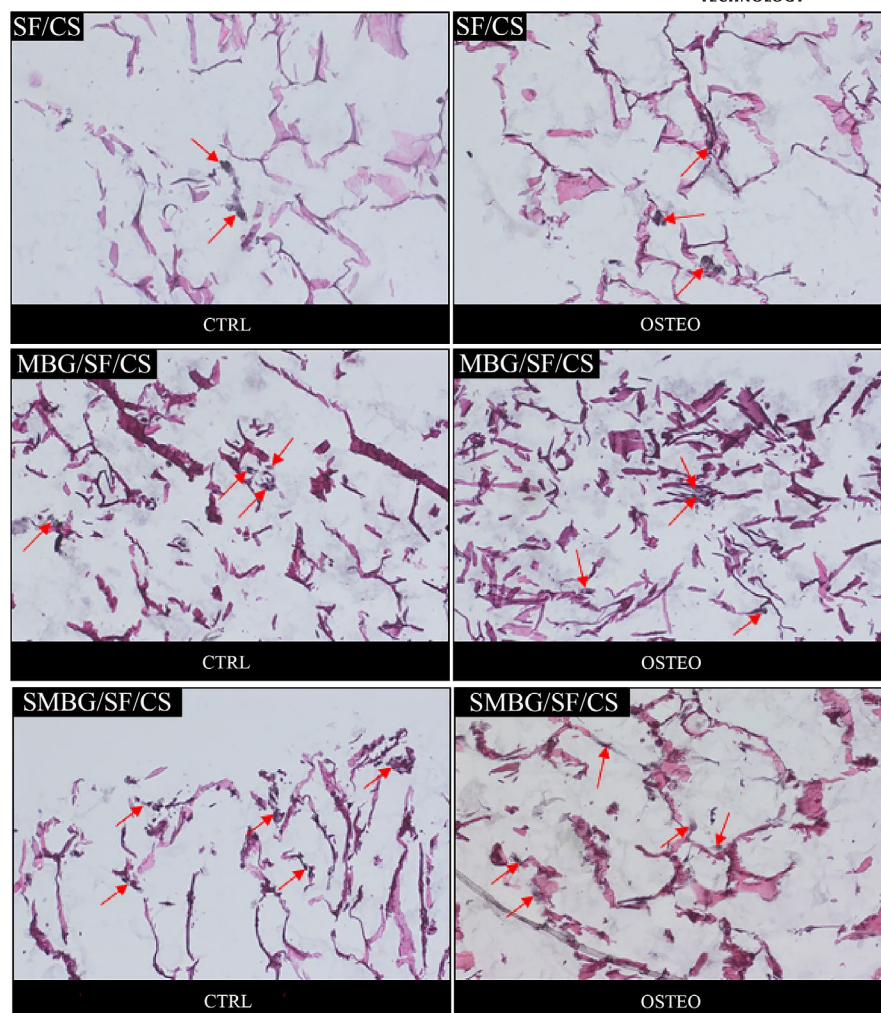
the mixture of chitosan and silk fibroin by doping with mesoporous bioactive glass particles and then fabricated by freeze-drying method to make the porous structure of the scaffold. The mixing of CS and SF solution resulted in the structural changes of silk fibroin from random coil to β-sheet structure.[23] The porosity of the composite scaffold plays an important role for bone tissue engineering, since it enables gas and nutrients exchange as well as cell migration and growth inside the scaffold. In this study, the percentage of porosity for the composite scaffolds was measured between 91.7% and 95.3%.

The MBG/SF/CS composite scaffold presented the highest porosity which could be explained by interference of large MBG particles to the structural formation of scaffolds compared to the others. From our previous work,[7,12] MBG presented an average particle size in the range of 26-48 μm while SMBG have smaller particle size (approximately 7-12 μm). The pseudo-wollastonite normally occurred at around 1125°C in the quenching techniques method. However, pseudo-wollastonite formation temperature could be lower than 1125°C because of the high reaction between starting precursors of the synthesized mesoporous bioactive glasses.[24]

Additionally, the crystallization of apatite and pseudo-wollastonite in silver-doped MBGMs may support biomineralization in osteoblast cell cultures and allows a strong bond between surfaces of the silver-incorporated MBGMs to bone. [25] The results showed that the doping with silver may favor the nucleation of pseudo-wollastonite and hydroxyapatite.

From Table 2, The porosity of SMBG/SF/CS composite scaffold was not significantly different from SF/CS scaffold. It can be hypothesized that small particle size and spherical shape of SMB homogenously dispersed in the SF/CS scaffold and did not affect the micro-environment architecture of the scaffolds.

More importantly, the incorporation of the mesoporous bioactive glass in SF/CS scaffolds led to improve the mechanical properties of scaffolds. The physical bonding between mesoporous glass particles and SF/CS mixture might occur due to the penetration of SF/CS solution into the pores of mesoporous bioactive glass particle.[26,27] The spherical morphology and uniformly small particle size distribution of SMBG led to a homogeneous dispersion into SF/CS solution. In this result, the mechanical properties of the composite scaffolds were quite lower than the previous reports.

The compressive strength of the composite scaffolds was in range of 0.3-0.45 MPa as compared to 1.5 MPa for trabecular bone[28] and 1.5-2.5 MPa for silk-chitosan scaffold from another report.[29] The compressive strength was found to have an inverse relationship with the pore size and porosity, which could be explained by a decrease in strut strength with increasing the pore size and porosity. From Figure 4, the decrease in pore sizes and the increase in wall thickness resulting from the combination of MBGs were responsible for the better mechanical properties in the composite scaffolds as compared to the silk/chitosan scaffold. However, the combination ratio of silk/chitosan and the concentration of silk, chitosan for the scaffold fabrication can be studied in the future to optimize the mechanical properties of the composite scaffolds.

In addition, the dispersion of mesoporous bioactive glass particles into SF/CS pore wall structure could affect the liquid absorption resulting to lower swelling ratio of scaffolds. The SF/CS scaffolds degraded quickly during the first 2 weeks.[30] Furthermore, the addition of mesoporous bioactive glasses could be used for controlling the degradation and bioactivity of scaffolds.

From ICP analysis, Ca and P ions concentration in SBF indicated the calcium phosphate deposition on the surface of the composite scaffolds as compared to the SF/CS scaffold. This result suggested that the addition of mesoporous bioactive glasses in scaffold could also improve the bioactivity of the composite scaffolds. Indeed, the calcium and phosphate ions released from bioactive glass during degradation could induce bone cell activity.[31] Chen et al evaluated the effect of different CaP-phases on the bone regeneration activity of Chitosan/CaP-membranes in vitro and in vivo. It was found that osteoblast cells increased adhesion and differentiation for CDHA phase while TCP provided its enhanced solubility thereby enhancing proliferation.[32]

hASCs exhibit several advantages in comparison to bone marrow MSCs. They possess a high proliferation rate and differentiative capacity, both toward angiogenic and osteogenic lineages.[33] This study indicated that SF/CS, MBG/SF/CS, and SMBG/SF/CS composite scaffolds could provide a suitable environment for hASCs with enough nutrition and gas exchange. Indeed, cells were able to grow and migrate inside the three scaffolds. Moreover, a proper osteogenic differentiation was always shown. The increase of alkaline phosphatase levels in these composite scaffolds might correlate with increased bone formation. In this perspective, the osteoinductive and osteoconductive performance of MBG/SF/CS scaffold was better than the others, even if they all shared a similar biocompatibility in terms of both cell viability and proliferation. This enhanced ALP activity of cells grown on MBG/SF/CS is most probably linked to its higher porosity, that allows a better metabolic exchange and therefore also a

deeper spreading inside the material of the osteogenic stimuli present in the culture medium. Thus, the result indicated that hASCs were able to adhere to mesoporous bioactive glass/SF/CS scaffolds and acquire an osteoblastic phenotype to produce the calcified extracellular matrix with important implications for tissue engineering.

5 | CONCLUSION

This study revealed a successful fabrication of mesoporous bioactive glass/silk fibroin/chitosan composite scaffolds allowing a good hASC viability, proliferation, and osteogenic differentiation. In vitro assays with hASCs revealed that all composite scaffolds showed good results regarding cytocompatibility, cell adhesion, and proliferation. However, the good biocompatibility result was achieved with SMBG/SF/CS scaffold. ALP activities of hASCs on both MBG/SF/CS and SMBG/SF/CS cultured in osteogenic medium were significantly higher compared with ones cultured on control medium suggesting that they allow a proper osteogenic differentiation. SMBG/SF/CS composite scaffolds offered a more suitable environment for cell attachment and proliferation and could be considered in the future as potential bone substitutes for hASCs cells transplantation in tissue engineering.

ORCID
Sirirat Tubsungnoen Rattanachan https://orcid.org/0000-0001-5241-7893

REFERENCES
1. Oryan A, Alidadi S, Moshiri A, Maffulli N. Bone regenerative medicine: classic options, novel strategies, and future directions. J Orthop Surg Res. 2014;9(1):18.
2. Saravanan S, Leena RS, Selvamurugan N. Chitosan based biocomposite scaffolds for bone tissue engineering. Int J Biol Macromol. 2016;93:1354–65.
3. Sharma K, Mujawar MA, Kaushik A. State-of-art functional biomaterials for tissue engineering. Front Mater. 2019;6:172.
4. She Z, Jin C, Huang Z, Zhang B, Feng Q, Xu Y. Silk fibroin/chitosan scaffold: preparation, characterization, and culture with HepG2 cell. J Mater Sci Mater Med. 2008;19(12):3545–53.
5. Li Z-H, Ji S-C, Wang Y-Z, Shen X-C, Liang H. Silk fibroin-based scaffolds for tissue engineering. Front Mater Sci. 2013;7(3):237–47.

PHETNIN ET AL.

Applied
Ceramic
TECHNOLOGY
International Journal of

2791

6. Pina S, Ribeiro VP, Marques CF, Maia FR, Silva TH, Reis RL, et al. Scaffolding strategies for tissue engineering and regenerative medicine applications. Materials. 2019;12(11):1824.

7. Phetnin R, Rattanachan ST. Bio-hybrid composite scaffold from silk fibroin/chitosan/mesoporous bioactive glass microspheres for tissue engineering applications. Adv Mat Res. 2016;1131:79–83.

8. Kargozar S, Montazerian M, Hamzehlou S, Kim HW, Baino F. Mesoporous bioactive glasses: promising platforms for antibacterial strategies. Acta Biomater. 2018;81:1–19.

9. Wu C, Zhang Y, Zhou Y, Fan W, Xiao Y. A comparative study of mesoporous glass/silk and non-mesoporous glass/silk scaffolds: physiochemistry and in vivo osteogenesis. Acta Biomater. 2011;7(5):2229–36.

10. Zuk PA, Zhu M, Mizuno H, Huang J, Futrell JW, Katz AJ, et al. Multilineage cells from human adipose tissue: implications for cell-based therapies. Tissue Eng. 2001;7(2):211–28.

11. Lee RH, Kim B, Choi I, Kim H, Choi H, Suh K, et al. Characterization and expression analysis of mesenchymal stem cells from human bone marrow and adipose tissue. Cell Physiol Biochem. 2004;14(4–6):311–24.

12. Phetnin R, Rattanachan ST. Preparation and antibacterial property on silver incorporated mesoporous bioactive glass microspheres. J Solgel Sci Technol. 2015;75(2):279–90.

13. Wu C, Chang J. Mesoporous bioactive glasses: structure characteristics, drug/growth factor delivery and bone regeneration application. Interface Focus. 2012;2(3):292–306.

14. Zhu M, Wang K, Mei J, Li C, Zhang J, Zheng W, et al. Fabrication of highly interconnected porous silk fibroin scaffolds for potential use as vascular grafts. Acta Biomater. 2014;10(5):2014–23.

15. Shahverdi S, Hajimiri M, Esfandiari MA, Larijani B, Atyabi F, Rajabiani A, et al. Fabrication and structure analysis of poly(lactide-co-glycolic acid)/silk fibroin hybrid scaffold for wound dressing applications. Int J Pharm. 2014;473(1):345–55.

16. She Z, Zhang B, Jin C, Feng Q, Xu Y. Preparation and in vitro degradation of porous three-dimensional silk fibroin/chitosan scaffold. Polym Degrad Stab. 2008;93(7):1316–22.

17. Bhardwaj N, Kundu SC. Silk fibroin protein and chitosan polyelectrolyte complex porous scaffolds for tissue engineering applications. Carbohydr Polym. 2011;85(2):325–33.

18. Bhardwaj N, Sow WT, Devi D, Ng KW, Mandal BB, Cho N-J. Silk fibroin–keratin based 3D scaffolds as a dermal substitute for skin tissue engineering. Integr Biol (Camb). 2014;7(1):53–63.

19. Kokubo T, Takadama H. How useful is SBF in predicting in vivo bone bioactivity? Biomaterials. 2006;27(15):2907–15.

20. Niada S, Giannasi C, Ferreira LMJ, Milani A, Arrigoni E, Brini AT. 17β-estradiol differently affects osteogenic differentiation of mesenchymal stem/stromal cells from adipose tissue and bone marrow. Differentiation. 2016;92(5):291–7.

21. Cocce V, Balducci L, Falchetti ML, Pascucci L, Ciusani E, Brini AT, et al. Fluorescent immortalized human adipose derived stromal cells (hASCs-TS/GFP+) for studying cell drug delivery mediated by microvesicles. Anticancer Agents Med Chem. 2017;17(11):1578–85.

22. Giannasi C, Pagni G, Polenghi C, Niada S, Manfredi B, Brini A, et al. Impact of dental implant surface modifications on adhesion and proliferation of primary human gingival keratinocytes and progenitor cells. Int J Periodontics Restorative Dent. 2018;3838:127–35.

23. Park SJ, Lee KY, Ha WS, Park SY. Structural changes and their effect on mechanical properties of silk fibroin/chitosan blends. J Appl Polym Sci. 1999;74(11):2571–5.

24. Ma J, Chen CZ, Wang D, Meng XG, Shi JZ. Influence of the sintering temperature on the structural feature and bioactivity of sol–gel derived SiO_2–CaO–P_2O_5 bioglass. Ceram Int. 2010;36:1911–6.

25. Sautier JM, Kokubo T, Ohtsuki T, Nefussi JR, Boulekbache H, Oboeuf M, et al. Bioactive glass-ceramic containing crystalline apatite and wollastonite initiates biomineralization in bone cell cultures. Calcif Tissue Int. 1994;55:458–66.

26. Peter M, Binulal NS, Soumya S, Nair SV, Furuike T, Tamura H, et al. Nanocomposite scaffolds of bioactive glass ceramic nanoparticles disseminated chitosan matrix for tissue engineering applications. Carbohydr Polym. 2010;79(2):284–9.

27. Tiyaboonchai W, Chomchalao P, Pongcharoen S, Sutheerawattananonda M, Sobhon P. Preparation and characterization of blended Bombyx mori silk fibroin scaffolds. Fiber Polym. 2011;12(3):324.

28. Kaur G, Kumar V, Baino F, Mauro JC, Pickrell G, Evans I. Mechanical properties of bioactive glasses, ceramics, glass-ceramics and composites: state-of-the-art review and future challenges. Mater Sci Eng. 2019;104:109895.

29. Teimouri A, Ebrahimi R, Chermahini AN, Emadi R. Fabrication and characterization of silk fibroin/chitosan/Nano γ-alumina composite scaffolds for tissue engineering applications. RSC Adv. 2015;5:27558–70.

30. Li J, Wang Q, Gu Y, Zhu Y, Chen L, Chen Y. Production of composite scaffold containing silk fibroin, chitosan, and gelatin for 3D Cell culture and bone tissue regeneration. Med Sci Monit. 2017;23:5311–20.

31. Kanatani M, Sugimoto T, Fukase M, Fujita T. Effect of elevated extracellular calcium on the proliferation of osteoblastic MC3T3-E1 cells: Its direct and indirect effects via monocytes. Biochem Biophys Res Commun. 1991;181(3):1425–30.

32. Chen Y-H, Tai H-Y, Fu E, Don T-M. Guided bone regeneration activity of different calcium phosphate/chitosan hybrid membranes. Int J Biol Macromol. 2019;126:159–69.

33. Paduano F, Marrelli M, Amantea M, Rengo C, Rengo S, Goldberg M, et al. Adipose tissue as a strategic source of mesenchymal stem cells in bone regeneration: a topical review on the most promising craniomaxillofacial applications. Int J Mol Sci. 2017;18(10):2140.